Structure and behavior of collagen fibers

11

Frederick H. Silver[1], *Michael Jaffe*[2], *Ruchit G. Shah*[1]
[1]Rutgers, The State University of New Jersey, Piscataway, NJ, United States;
[2]NJIT, University Heights, NJ, United States

11.1 Introduction

Collagen fibers form the basic structural components of the extracellular matrix (ECM) of vertebrates that serve to store elastic energy during muscular deformation, transmit stored energy into joint movement, and transfer excess energy from the joint back to the attached muscles for dissipation (Silver and Landis, 2008). They also act as mechanotransducers by transferring stress borne by the musculoskeleton to the attached cells in order to regulate tissue metabolism, either up or down, as a result of changes in mechanical loading (Silver, 2006). Finally, they prevent premature mechanical failure of tissues and limit deformation of most ECMs and organs (Dunn and Silver, 1983). Therefore, the collagen fiber structure is intimately related to energy storage, transmission and dissipation, and premature mechanical failure of tissues.

Collagen fibers are composed of collagen triple-helical molecules that are derived from one or more of the 28 collagen types that compose the collagen family (Ricard-Blum, 2011). The collagen family is composed of collagen subfamilies including fibril-forming collagens, beaded filaments, anchoring fibrils, and networks. Most collagen fibrils are composites since they are made up of more than one collagen type such as tendon (types I, II, and V), cartilage (types II, IX, and XI), skin (types I and III), and cornea (types I, III, and V). In addition, other noncollagenous macromolecules are attached to collagen fibrils that are involved in fibril formation (proteoglycans), cell-collagen interactions (fibronectin), and mechanotransduction (integrins) (Ricard-Blum, 2011).

11.2 Collagen molecular structure

The chemical description of collagen is a protein containing three polypeptide chains, each of which is composed of one or more regions containing the sequence Gly-X-Y, where X and Y can be any other amino acid residue but is commonly proline and hydroxyproline, respectively. This three-chained molecule forms a right-handed triple helical structure containing glycine residues buried at the center of the cylindrical molecule and is synthesized in a longer precursor form termed procollagen (see Fig. 11.1). The most abundant subfamily is the fibrillar collagens of which type I

Handbook of Properties of Textile and Technical Fibres. https://doi.org/10.1016/B978-0-08-101272-7.00011-0

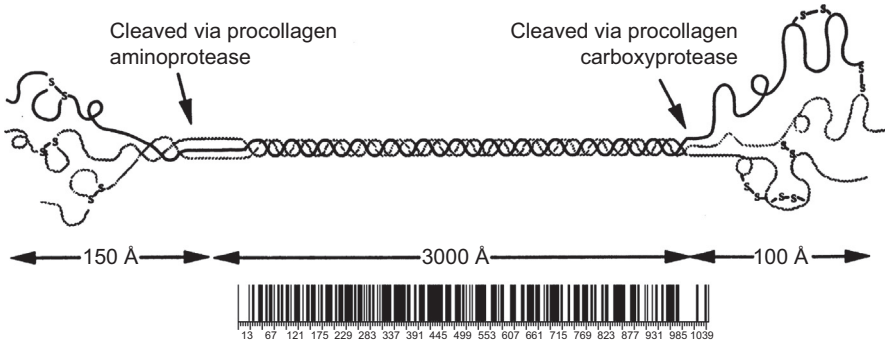

Figure 11.1 This diagram illustrates the structure of procollagen, the biosynthetic precursor of the collagen molecule. Procollagen molecules are formed within the cell and the large propeptides are cleaved extracellularly during self-assembly into crosslinked collagen fibers. Collagen molecules are triple helical rods about 300 nm in length as shown by the arrows in the diagram. The flexibility profile is shown below the diagram of the collagen triple helix and the 300 nm (3000 Å) line that represents the triple helical portion. The *dark vertical lines* represent rigid regions and the light areas depict the flexible domains of the collagen triple helix at the bottom of the figure. The amino acid residue numbers along the axis of the triple helical collagen molecule are shown at the bottom of the flexibility profile. The collagen triple helix is flexible at the molecular level since the light regions depicted in the figure do not contain proline and hydroxyproline. The two imino acids contain rings prevent the formation of a rigid triple helix. Upon tensile loading the flexible domains stretch, storing mechanical energy that can later be transmitted to joints to allow movement such as locomotion.

collagen is found in tendons, skin, cornea, bone, lung, and vessel walls (Hulmes, 2008). This collagen is thought to give rise to the high tensile strength of collagen fibers in tendon; in addition, it actively is involved in other physiologic processes such as mechanotransduction.

Collagen synthesis from amino acids begins on the ribosomes within the cell cytoplasm; it is then folded into a triple helix after hydroxylation of proline is completed. The molecules are then transported through the Golgi apparatus, packaged into vesicles, and then are added to growing fibrils in recesses within the cell membrane. However, collagen fibrils are not mechanically stabilized until they are cross-linked, which occurs after release from the cell and mechanical loading begins (McBride et al., 1985, 1988).

Procollagen is in the form of a triple helix (Fig. 11.1) with extra pieces on the ends termed propeptides. The propeptides are removed sequentially during collagen assembly. Collagen triple helices, 1.5 nm wide and 300 nm long, are packed into a "quarter-staggered" packing pattern that results in nearest neighboring molecules being staggered longitudinally by about 22% of their molecular lengths with a space or hole between the head of one molecule and the tail of the next (Fig. 11.2) (see Silver et al., 2003 for a review). Early studies recognized that five collagen molecules were packed in staggered fashion to form a microfibril (Smith, 1968; Doyle et al., 1974) that was identified by electron microscopy (Pease and Bouteille, 1972). We now believe

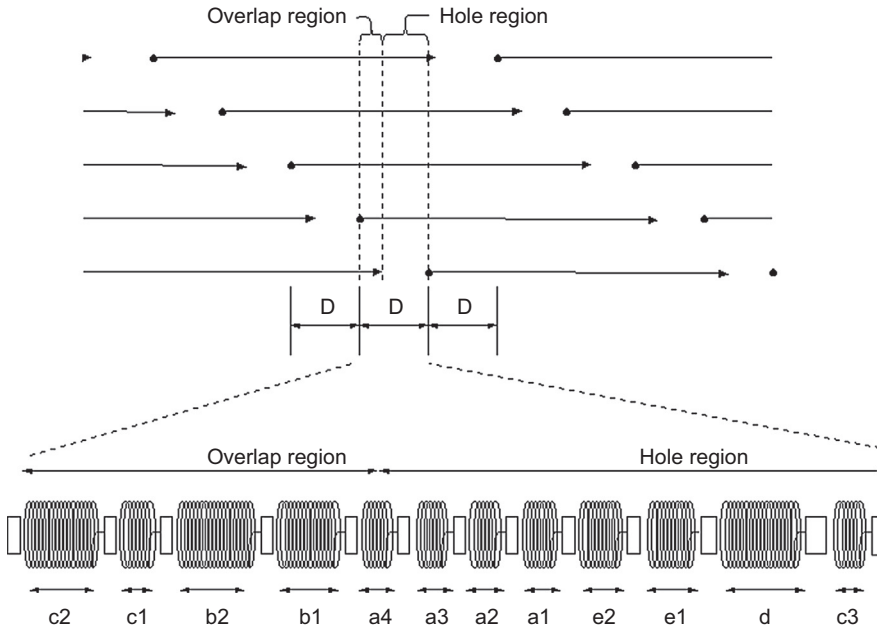

Figure 11.2 The top portion of this figure illustrates the structure of a five-membered microfibrillar unit that is believed to be the repeat unit found in collagen fibrils and fibers and appears as a quasi-hexagonal unit by X-ray diffraction of tendon. In this packing pattern five collagen molecules are staggered by about 22% of the molecular length of 300 nm with respect to their nearest neighbors. A space or hole 0.6 D in length (D is between 64 and 67 nm) is left between neighboring molecules. The collagen molecule is 4.4 D long where D is the stagger between neighboring collagen molecules. The distance D consists of an overlap zone of 0.4 D and a hole region of 0.6 D as is shown by the *vertical dotted lines* that are superimposed on the microfibril in the diagram. The overlap and hole regions that make up the D repeat consist of 13 rigid and 12 flexible domains in the expanded view at the bottom of the figure and are depicted by the rectangles and springs shown, respectively. The 12 flexible regions are identical to the 12 bands denoted c2 through c3 (see Fig. 11.3(d,e)) that are seen as dark vertical lines across the collagen fibril when collagen is stained with heavy metals and viewed in the electron microscope. The 12 flexible regions are believed to be stretched when collagen fibrils are initially mechanically deformed reflecting experimental increases in the axial rise per amino acid residue, h spacing, that are observed by X-ray diffraction. Further loading causes increases in the D period and molecular and fibrillar slippage. Collagen molecules in tendon are held together in the microfibril with crosslinks that occur at the tail of one molecule (see *circle*) to the head of a lateral neighboring molecule (see *arrowhead*). These crosslinks are staggered by a distance of 4D.

that collagen molecules are packed laterally into a quarter-staggered or quasi-hexagonal unit that is in turn longitudinally packed into microfibrils. Collagen microfibrils are believed to be continuous and run the length of a tissue and are fused laterally into fibrils and fibers in most tissues (Silver et al., 2003).

In the 1970s, collagen molecule was thought to be a rigid rod based on the observation that the translational diffusion constant was 0.86×10^{-6} cm^2/s, which was very close to that calculated for a prolate ellipsoid 1.5 nm wide and 300 nm long (Silver et al., 1979). However, later measurements, based on rotary shadowed images of collagen molecules, suggested that the molecules had numerous bends as shown in Fig. 11.3 (Birk et al., 1991). Analysis of the molecular sequence of type I, II, and III collagens suggested that the flexibility of the collagen triple helix arises from areas in the sequence that are devoid of proline and hydroxyproline, two imino acids that constrain rotation and flexibility of the molecule (Silver et al., 2003) (see Fig. 11.2).

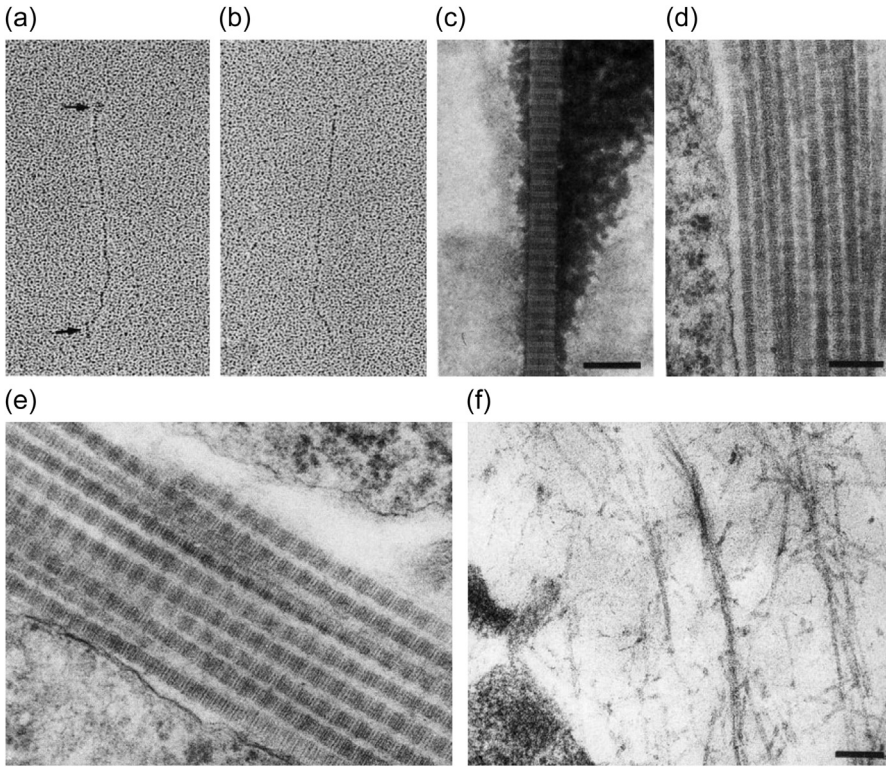

Figure 11.3 Structural hierarchy of collagen in ECMs. Collagen molecules are semiflexible rods (see bends in a, b) in rotary shadowed transmission electron microscope images, that form cross-striated fibrils in tissues with repeat periods between 64 and 67 nm (c–e) or filamentous structures (f). Collagen fibrils are formed in deep recesses of the cell membrane (g, h) and under polarized light appear as planar biaxial structures in dermis (i), orthogonal structures in bone (see *arrows* for collagen molecular directions in j), and crimped planar waveforms in tendon (k). This figure was modified from Birk et al. (1991). The nonlinear viscoelastic behavior of collagen fibers is due to the collagen fibril orientation and the presence of other structural components such as elastic fibers and the presence of crimp.
Cell Biology ECM, Springer.

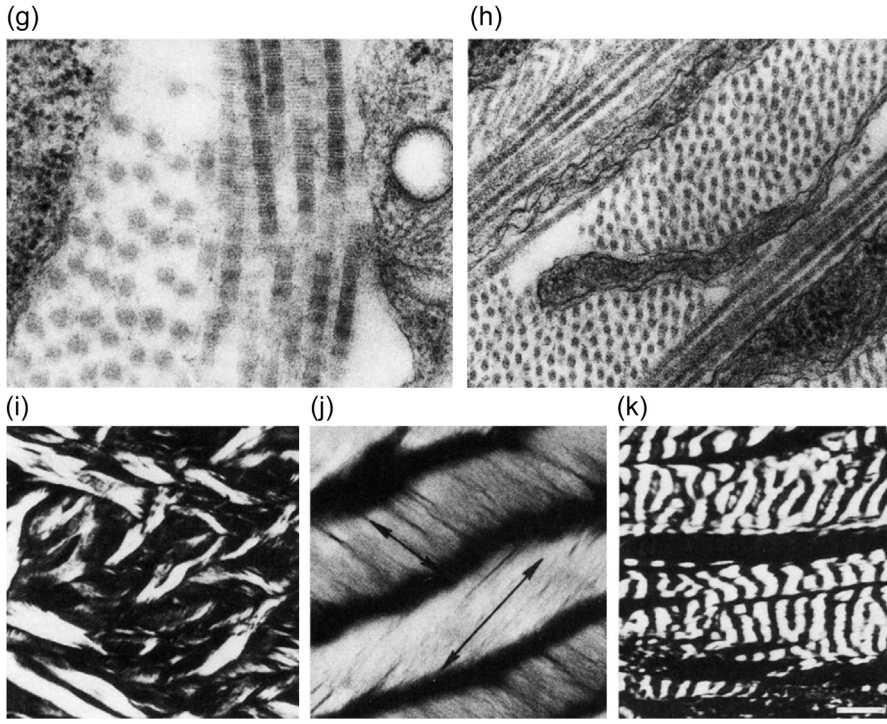

Figure 11.3 cont'd.

Further analysis suggested that these flexible regions are preserved when the molecules are packed into a quasi-hexagonal packing pattern suggesting that the flexibility is an important aspect of the collagen fibril structure (Silver et al., 2002).

11.3 Supramolecular structure of collagen

Collagen in tissues is recognized by transmission microscopy by its regular repeat of the charged amino acid residues. In the quarter-staggered packing pattern, the amino acid sequence of the five molecules in cross-section is repeated every 64−67 nm, a distance termed the D period (Fig. 11.2). The positively stained sub-bands in the D period can be depicted as springlike (see Fig. 11.2) and can be directly visualized by staining with heavy metals (see Fig. 11.3). The D period varies from about 64 to 67 nm depending on the tissue of origin. In tendon, the D period is about 64 nm and in skin it is about 67 nm (see Fig. 11.3(c−e)). At the light microscopic level, collagen fibers in tendon are distinguished from other tissue proteins by the cross-striated pattern derived from the crimp seen under polarized light (Fig. 11.3(k)). Other tissues contain collagen fibers in aligned (tendon) and oriented networks that are visualized under polarized light (see Fig. 11.3).

For instance, in tendon, collagen fibril diameters are between 20 and 280 nm and collagen fibers have diameters between 1 and 300 μm (Silver et al., 2003). While collagen fibrils form from lateral addition of smaller fibrils (see Fig. 11.3), they form bundles of fibrils and larger bundles termed fascicles as shown in Fig. 11.4. Groups of fibril bundles form fascicles that in turn make up the cross-section of a tendon bundle (Fig. 11.4). These structural elements acting in concert give rise to the mechanical properties of tendon.

The ultrastructure of tendon has been studied extensively as a function of maturation (Torp et al., 1974; Parry et al., 1978). Collagen microfibrils appeared to be held together by an interfibrillar matrix containing proteoglycans (Scott, 1992). These collagen fibrils were observed to have a planar waveform, termed crimp, and be the load-bearing units (Diamant et al., 1972) (Fig. 11.3(k)). Upon deformation, the stress–strain curve of tendon curves upward after the crimp is removed (Diamant et al., 1972). After birth, the distribution of fibril diameters from rat tail tendons is fairly flat supporting the concept that fibril diameter and length increases occur by the lateral fusion of fibril bundles (Torp et al., 1974; McBride et al., 1985, 1988; Birk et al., 1991). The volume fraction of collagen fibrils increases during maturation until it reaches about 0.5; in fibril cross-sections of tendon small collagen fibrils fill the space between larger ones (Torp et al., 1974).

11.4 Collagen crosslinking

The ability of fibril-forming collagens to store, transmit, and dissipate energy requires crosslink formation between molecules within a microfibril and between microfibrils and other structural units. These crosslinks include lysine and hydroxylysine derivatives and other amino acid residues including histidine (Silver et al., 1992). Crosslinking also occurs during aging and involves glucose molecules (Ricard-Blum, 2011). The stiffening and poor energy dissipation of collagen fibers associated with aging probably involves collagen fiber fragmentation by ultraviolet light and glucose-derived crosslinking. This leads to loss of the energy dissipating ability of ECM and is associated with large energy losses during pulsatile blood flow in the cardiovascular system (Horvath et al., 2005).

11.5 Collagen self-assembly

Collagen molecules self-assemble under physiological conditions into a quarter-staggered structure, the microfibril, that in turn grows linearly and laterally into collagen fibrils (Silver et al., 2003). Collagen triple helices and microfibrils are very long and thin and are therefore quite flexible. Solution studies suggest that the collagen molecule can be modeled as a semiflexible rod with bend angles up to about 120 degrees with respect to the molecular axis (Silver et al., 2003). This flexibility allows collagen molecules to undergo conformational changes required for self-assembly into long thin fibrils via end-overlap of several molecules followed by lateral assembly

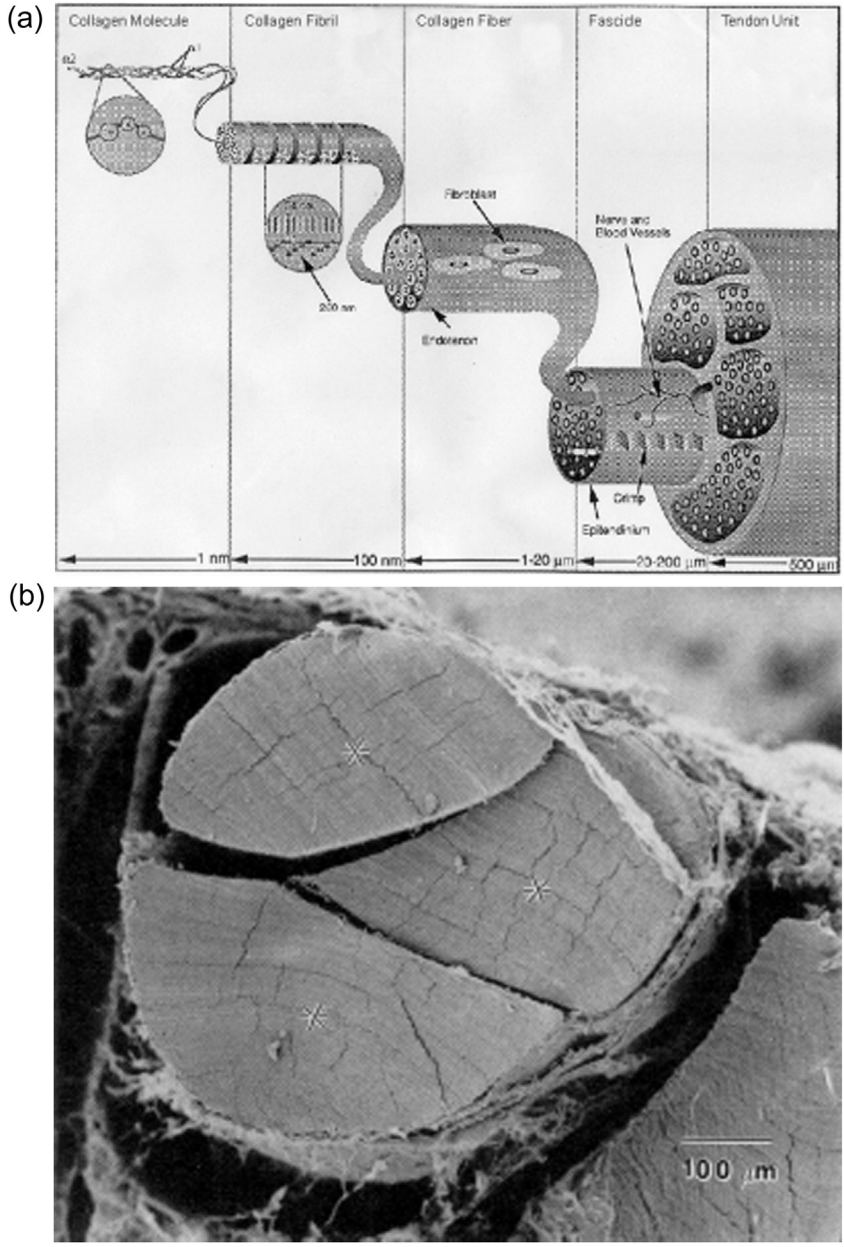

Figure 11.4 Structural hierarchy in the tendon. (a) This diagram illustrates the relationship between collagen molecules, fibrils, fibers, fascicles, and tendon units. Although the diagram does not show fibril subunits, collagen fibrils appear to be self-assembled from intermediates integrated within the fibril termed microfibrils. (b) Scanning electron micrograph of a rat-tail tendon fiber showing the fascicles (see *asterisks*) that make up the tendon unit. Tendons in humans contain many fascicular units.

into microfibrils with diameters that are multiples of 4 nm. The flexibility of collagen molecules and fibrils allows both load transmission and energy storage (Silver, 2006).

The ability of collagen molecules to self-assemble into fibrils occurs not only in tissues but also in vitro. The self-assembly of collagen molecules from solutions of type I collagen is a model that has been used to understand the structure and mechanical behavior of collagen fibers in tissues. Results of self-assembly studies in vitro have shown that crosslinking is a very important step in converting collagen fibers that deform primarily in a viscous fashion into energy storing elements (Silver et al., 2000).

11.6 Viscoelastic behavior of collagen fibers

Collagen fibers are viscoelastic and exhibit time-dependent mechanical behavior (Fig. 11.5). Viscoelasticity may be important in resisting impact loads especially in the musculoskeleton; however, it complicates the understanding of ECM behavior since most real-time measurements made on these tissues contain both elastic and viscous contributions (Dunn and Silver, 1983). The elastic behavior varies from as high as about 75% of the total stress for tendon to as low as about 50% for skin

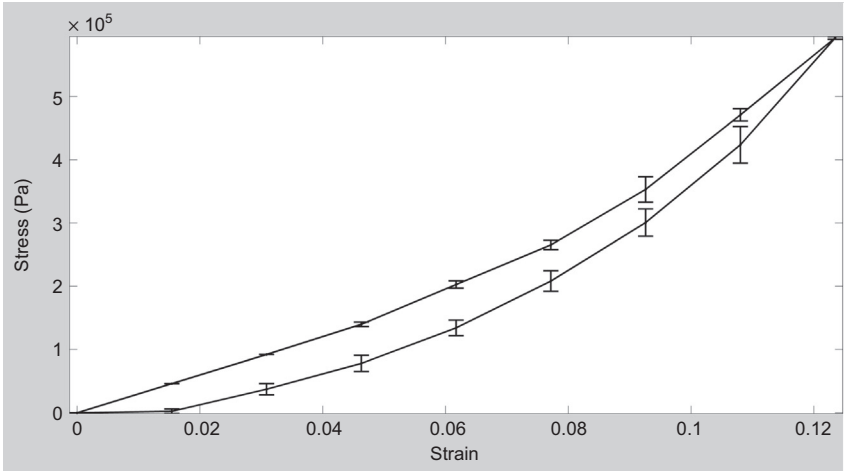

Figure 11.5 Tensile stress−strain curve for decellularized dermis. The loading (upper curve) and unloading curves (lower curve) for decellularized human dermis tested uniaxial tension are shown. The loading curve is above the unloading curve due to energy loss during the cycle. The unloading curve does not recover immediately but returns to zero strain after a recovery time of about 30 min. This time dependence of the recovery strain is a manifestation of the viscoelasticity of human dermis. The time dependence of the mechanical properties of ECMs is manifested by the strain-rate dependence of the stress−strain curve, the recovery time for the sample to achieve zero strain, and the dependence of the modulus on the strain-rate. The modulus of collagenous tissues is time and strain-rate dependent and varies from about 0.5 MPa for cardiovascular tissue to over 20 GPA for bone.

depending on the collagen fiber orientation, rate of loading, and the quantity of other tissue constituents (Dunn and Silver, 1983).

A number of excellent studies have been published that have helped in the interpretation of the stress−strain behavior of tendon at the molecular and fibrillar levels. Much of our current understanding of the relationship between hierarchical structure and viscoelastic behavior of ECMs is based on studies of the mechanical properties of developing and mature tendons (Torp et al., 1974; McBride et al., 1985, 1988). The properties of developing tendon rapidly change just prior to the onset of locomotion. The maximum total stress that can be borne by a 14-day-old embryonic chick leg extensor tendon is about 2 MPa and increases to 60 MPa, 2 days after birth (McBride et al., 1985, 1988). This rapid increase in tensile stress by tendon occurs without large changes in its hierarchical structure (McBride et al., 1985, 1988). In this case, the collagen fibril length appears to be more important for energy storage and for increased ultimate tensile strength than fibril diameter; but the two parameters are linked together since fibrils have been shown to grow in length by lateral fusion of fibril bundles (Torp et al., 1974; McBride et al., 1988; Silver et al., 2003).

Mechanistically, during mechanical loading, a tensional increase in the D period is observed with increasing strain that is associated with (1) molecular elongation at the triple-helical level of structure; (2) increases in the gap distance between the end of one triple-helix and the start of the next one in the microfibril (see Fig. 11.2); and (3) molecular slippage (Sasaki et al., 1999). Molecular stretching occurs at lower stresses followed by increases in the gap spacing and molecular sliding that occur at higher stresses (Folkhard et al., 1987).

The time-dependent behavior of tendon makes it difficult to interpret stress−strain relationships for these tissues. However, using incremental stress−strain curves, the elastic and viscous behaviors can be separated and analyzed in terms of tissue structure (Dunn and Silver, 1983). The viscoelastic properties of ECMs have been obtained by constructing incremental stress−strain curves for a variety of tissues including tendon (Dunn and Silver, 1983; Silver, 2006) (see Fig. 11.6 top). Such incremental stress-strain curves are derived for tendon and other ECMs by stretching the tissue in a series of strain increments and then allowing the stress to relax to an equilibrium value at each strain increment before another strain increment is added (Fig. 11.6 top) (Dunn and Silver, 1983). By subtracting the elastic stress (equilibrium stress value) from the initial or total stress value, the viscous stress is obtained. By plotting the equilibrium stress versus strain and the total stress minus the equilibrium stress versus strain (Fig. 11.6 bottom) we get elastic and viscous stress−strain curves for tendon (Silver, 2006) (Fig. 11.7). From these curves and the literature, important information can be obtained concerning the mechanism of stretching and sliding of the collagen molecules and fibrils that make up the structure of tendon (Silver, 2006). It turns out that the slope of the elastic stress−strain curve is proportional to the elastic modulus of the collagen molecule (Silver et al., 2003), while the viscous stress at a particular strain is a measure of the fibril length (Silver et al., 2003). An estimate of the elastic modulus of the collagen molecule is obtained by dividing the slope of the elastic stress−strain curve by the collagen content and by the ratio of the molecular strain (change in h spacing-axial rise per amino acid residue along the molecule backbone) divided by the

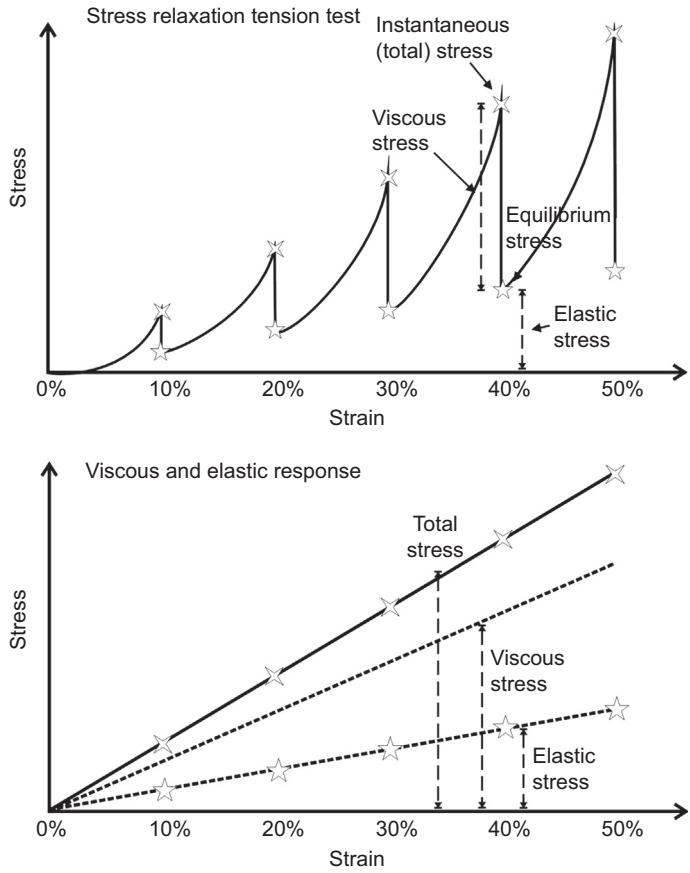

Figure 11.6 Incremental stress−strain curves for ECMs tested in tension. (Top) A strain increment is applied to the ECM and the initial stress is measured. The strain increment varies from about 2% for tendon to about 10% for skin. The stress is allowed to relax at room temperature until an equilibrium value is reached. The process is repeated until the sample fails. (Bottom) Plots of all the initial (total) and equilibrium stresses are made versus strain as well as plot of the total minus equilibrium stress versus strain. The equilibrium stress versus strain curve is equivalent to the elastic stress−strain curve while the difference between the total and equilibrium stress is the viscous stress. The elastic stress−strain curve has been found to be independent of strain-rate for skin, tendon, and cartilage while the viscous contribution increases with increasing strain-rate.

macroscopic strain (0.1 for tendon) (Silver, 2006). Using this approach a value between 7 and 9 GPa for the elastic modulus of the collagen molecule is found for rat tail tendon collagen (Silver, 2006) (see Table 11.1). Collagen fibril lengths calculated from the viscous stress and hydrodynamic theory (Silver, 2006) range from about 20 μm for developing tendon to in excess of 1 mm for adult tendons as shown in Table 11.2 (Silver, 2006).

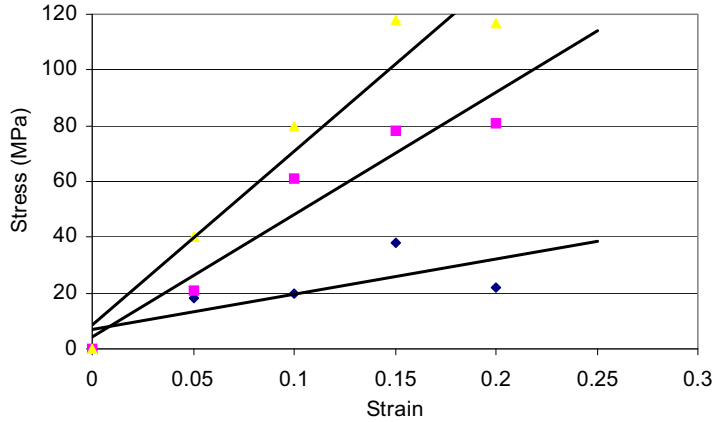

Figure 11.7 Total, elastic and viscous stress−strain curves for rat tail tendon fibers obtained after incremental stress−strain testing in uniaxial tension. This figure shows that the elastic stress−strain curve (*squares*) is approximately linear with strain and is above the viscous curve (*triangles*). This diagram illustrates that more energy is stored during tensile deformation of tendon than is dissipated as heat during stretching.

Table 11.1 Estimated elastic moduli for collagen based on elastic stress measurements for various ECMs

Molecule	Tissue	Elastic modulus (GPa)
Type I	Self-assembled	6.51
	Rat tail tendon	7.69
	Turkey tendon	4.20 (no mineral)
		7.22 (mineral 0.245)
Types I and III	Skin	4.4
Type II	Articular cartilage	7.0 (surface parallel)
		2.21 (surface perpendicular)
		4.91(whole parallel)
		1.52 (whole perpendicular)
	Osteoarthritic cartilage	0.092 (whole perpendicular)
Elastin	Skin	0.040
	Vessel wall	0.01

Table 11.2 Estimated collagen fibril lengths based on mechanical measurements of viscous loss in different ECMs

Tissue		Fibril length (mm)
Rat tail tendon		0.860
Self-assembled collagen fibers		0.0373
Turkey tendon	(no mineral)	0.108
Turkey tendon	(0.245 mineral content)	0.575
Human skin		0.0548
Articular cartilage	(surface parallel)	1.265
	(surface perpendicular)	0.688
	(whole parallel)	0.932
	(whole perpendicular)	0.696
Osteoarthritic	(whole perpendicular)	0.164

11.7 Viscoelasticity of self-assembled type I collagen fibers

Additional information concerning the deformation mechanisms of tendon can be derived from understanding the behavior of model systems such as self-assembled type I collagen fibers derived from solubilized rat tail tendon collagen. The fibers are self-assembled under conditions that produce D-banded collagen fibrils similar to those seen in rat tail tendons (Silver et al., 2000, 2001). The purified type I collagen fibrils produced by self-assembly are much narrower than those observed in tendon, e.g., between about 20 and 40 nm in diameter, as compared to those in tendon that are as large as several mm. Incremental stress−strain curves for self-assembled purified type I collagen are approximately linear for uncrosslinked collagen fibers (Silver et al., 2000, 2001). However, unlike the incremental stress−strain curves for rat tail tendon, the viscous stress−strain curve for uncrosslinked self-assembled collagen fibers is above the elastic stress−strain curve (Silver et al., 2001). This result suggests that in the absence of crosslinks, the ability of collagen fibers to transmit tensile forces is impaired; transmission of tensile forces appears increased by the formation of crosslinks (Silver, 2006). When the self-assembled collagen fibers are subsequently crosslinked by aging at room temperature, the elastic stress−strain curve is then above the viscous one (Silver et al., 2001). Comparison of the slopes of the elastic stress−strain curves for tendon and self-assembled collagen fibrils, suggests that the slope of the elastic stress−strain curve for crosslinked self-assembled collagen fibrils is much closer to that of tendon than is the slope for uncrosslinked collagen fibers (Silver, 2006). This result underscores the need for end-to-end crosslinking between collagen

molecules in order to facilitate tensile force transmission during stretching (Silver, 2006) (see Fig. 11.2). The tensile properties of tendon and crosslinked self-assembled collagen fibers are very similar. The major difference is that the diameters of self-assembled collagen fibrils are much smaller than the diameters of collagen fibrils found in tendon. The transmission of tensile forces by tendon is attributable to direct stretching of the triple helix; energy loss occurs through the sliding of fibrils and bundles of fibrils during tensile deformation. The behavior of other ECMs is a bit more complicated than that of self-assembled collagen fibers because of the presence of additional components including elastic and smooth muscle fibers and differences in collagen fiber orientation (Silver, 2006).

Morphologic studies on collagen fibers suggest that mechanical deformation leads to collagen fibril alignment as well as development of fibril substructure that affect the failure mechanisms of collagen fibers (Pins et al., 1997). Stretching during self-assembly results in collagen fibers, with the outer fibrils containing additional axial orientation and a more prominent fibrillar substructure compared to fibrils found in the center of the fiber (Pins et al., 1997). Stretching during self-assembly also leads to increased ultimate tensile strengths and axial alignment of the collagen subfibrils (Pins et al., 1997). Stretched uncrosslinked collagen fibers require more energy to pull to failure and the failed fiber surface shows more plastic deformation than does the fracture surfaces of unstretched collagen fibers (Pins et al., 1997).

11.8 Collagen fiber failure

The effects of cycling on the structure of collagen fibrils in tendon have been reported in the literature (Torp et al., 1974). Repeated mechanical cycling leads to the formation of voids within collagen fibrils (Torp et al., 1974). Dissociation of fibrils starts in spots where voids are seen and results in the observation of 15 nm in diameter subunits that lack the collagen D-period (Torp et al., 1974). Fissures become apparent under repeated tensile loading at sites where fibroblasts are in contact with the collagen fibrils. Collagen fibril failure is reported to occur primarily by progressive dissociation into subfibrils, 15 nm in diameter, with some loss of the axial alignment of the fibrils. In addition, a secondary mechanism of failure is observed in rats 1.5 months and older. Fibroblasts in tendons from this age group appear to develop fissures that eventually extend to other fibroblasts leading to tendon failure (Torp et al., 1974). The improved failure stress observed with increased age appears to be a result of increased crosslinking that leads to reduced slippage between the subfibils and microfibrils (Torp et al., 1974).

While macroscopic fiber failure is quite apparent since visible fiber breakage can be observed, subfiber failure has been observed and attempts have been made to quantitatively analyze these changes based on observed behavioral differences. Subfiber failure can be used to examine a number of altered mechanical phenomena in tendons and ligaments including increased laxity (Panjabi et al., 1996; Provenzano et al., 2002a,b) and decreased stiffness (Panjabi et al., 1999; Provenzano et al., 2002a,b). Subfiber failure leads to collagen disorganization (Torp et al., 1974; McBride et al., 1985, 1988),

fibroblast necrosis (Provenzano et al., 2002a,b), and altered collagen fiber orientation. At the macroscopic level collagen fiber failure in tendon has a distinct morphological character.

Statistical analyses indicate that the onset of subfiber failure occurs at a strain of about 5% in a ligament that is below the threshold for structural damage (Provenzano et al., 2002a,b). Cellular damage induced by ligament sprains occurs at strains significantly below failure strains (Provenzano et al., 2002a,b). Subfiber failure appears to be associated with altered collagen fiber rotation during tissue extension. While tissue remodeling and synthesis of collagen types I and III can occur at subfailure strains through fibroblast mediated processes, the pre-subfailure strengths of ligaments are never regained and permanent joint laxity occurs (Provenzano et al., 2002a,b, 2005). Subfiber failure is first observed in thin diameter collagen fibrils followed by failure of the larger diameter collagen fibrils (Yahia et al., 1990). Ker (2008) has reviewed the macroscopic fracture mechanics of tendon. When a tendon is notched laterally and loaded in tension longitudinally, the crack opens up and the tip becomes curved. Since the ratio of the shear modulus to that of the tensile modulus of tendon is about 10^{-3}, the crack propagates longitudinally and leads to a mode of failure called "interdigitation." This failure surface is characterized by the presence of numerous collagen fibrils that one by one tear at different lengths and morphologically look like series of fingers projecting across the failed tendon ends. Ker et al. (2000) reported a correlation between stress-in-life (physiological operating stress levels) and resistance to fatigue damage leading to the conclusion that all tendons are equally likely to experience damage independent of their normal operating stresses. Ker (Ker, 2008; Ker et al., 2000) further hypothesized that damage of tendon during normal loading acts to trigger tendon repair processes and that tendon damage and failure are limited by the weakness of the attached muscle.

11.9 Nondestructive methods for studying mechanical behavior of collagen fibers and tissues

The ability to monitor the mechanical properties of collagen and ECMs in vivo is an important measurement needed for early diagnosis of disease and the ability to follow disease progression. The ability of physicians to "palpate" changes in the properties of tissues associated with tumors and calcification suggests that there are major changes in the structure and properties of collagen and ECMs during disease processes. It is essential that clinicians be able to assess the changes at the collagen fibril and fiber levels of structure to accurately diagnose and treat diseases such as cancer. Several new methods have been developed to try and discern these changes early in the disease process. It is essential that these methods be validated so that the properties measured have some meaning.

There are several fairly new methods that have been evaluated in the literature to study the mechanical properties of tissues in vivo such as magnetic resonance elastography (MRE), ultrasound elastography (UE), optical coherence tomography (OCT),

ocular response analyzer (ORA), optical coherence elastography (OCE), and OCT with vibrational analysis that are quite promising. Classical methods such as constant rate-of-strain deformation as well as incremental stress−strain analysis are useful but prove to be too destructive to tissue and therefore have limited value for measuring tissue properties in vivo.

11.9.1 Magnetic resonance elastography

MRE has been used to calculate values of the modulus of tissues. In this method, mechanical excitation is produced by pneumatic, electromechanical, or piezoelectric stimulators positioned next to the body (Low et al., 2016). The tissue is loaded by one of these means and then the magnetic resonance imaging (MRI) signal is collected. The phase shift in the MRI signal is used to calculate a value of the modulus; however, the workers assume that Poisson's ratio is 0.5 and that the tissue density is 1.0 g/cc. These assumptions create calculation errors since Poisson's ratio has been shown to vary from 0.5 for tissues (Shah et al., 2016). The value of this technique is that it can be used noninvasively in real time; however, use of this technique requires correction for Poisson's ratio and strain-rate effects to be entirely accurate.

11.9.2 Ocular response analyzer

The ORA is a clinical device that uses a high-speed air puff to deform the cornea. Changes in shape of the anterior surface are tracked using an infrared beam reflected from the surface and aligned with the geometry of a detector (see Ruberti et al., 2014 for a review). In this technique, corneal deformation is tracked after the air puff is applied to the corneal surface. Differences in the pressures between the inward and outward flattening of the cornea are reported as the corneal hysteresis. Changes in the corneal hysteresis are correlated with disease states anecdotally. The noninvasiveness of this technique is a positive attribute of this method. However, the inability to relate the results to standard mechanical testing parameters limits the utility of this method.

11.9.3 Optical coherence elastography

OCE has been used for the analysis of tissue mechanical properties (Kennedy et al., 2014a,b; Wang and Larin, 2015). This technique uses light that is reflected off a surface and compared to the nonreflected light to create an image; the image is used to measure displacement after the tissue undergoes a small deformation. Mathematical modeling is used to calculate the tissue modulus assuming the tissue is a linear elastic solid and that Poisson's ratio is 0.5. This technique is noninvasive and can be used to evaluate tissue in situ. However, the values of moduli obtained from the models used appear lower than those calculated from destructive testing, suggesting that the strains introduced are not large enough to deform the collagenous components of the tissue.

11.9.4 Ultrasound elastography

Ultrasound elastography is referred to by a number of terms including strain elastography, compression elastography, sonoelastography, and real-time elastography (Drakonaki et al., 2012). Using these techniques a low-frequency compression is applied to the tissue, frequently via the hand held transducer. The applied compression induces a strain and the modulus is estimated from the change in the echo before and after the force is applied. Zaleska-Dorobisz et al. (2014) review the use of ultrasound to calculate the modulus values of tissues for different clinical applications. This technique assumes that the tissue is a linearly elastic solid that has a Poisson's ratio of 0.5; the technique does not measure the modulus directly. Clinically, this technique has been used to identify pathologic changes in a number of diseases. However, the data obtained from UE will depend on the frequency of sound used in the measurements and the assumptions made in converting the displacement to elastic modulus.

11.9.5 Vibrational analysis and optical coherence tomography

Pulsed laser excitation has been used to create a surface wave and estimate the modulus; this is accomplished using an equation that relates the surface wave velocity to the modulus. Song et al. (2015) used ultrasound to create a shear wave and used OCE to measure the properties of tissue. The above studies assumed a value for Poisson's ratio and a density to calculate the mechanical properties. The assumption of a value of 0.49 for Poisson's ratio leads to calculation errors as discussed above. These methods are noninvasive and if modified to correct for viscoelasticity and incompressibility would give improved results.

Shah et al. (2016) used vibrational analysis in concert with OCT to measure the resonant frequency of decellularized human dermis (Fig. 11.8). They applied an acoustic vibration to the samples under tension and showed that the resonant frequency squared obtained from the change in frequency of the reflected light was directly related with the tensile modulus obtained in an incremental stress−strain experiment (Fig. 11.9). Their method did not rely on the assumption of a value of Poisson's ratio; this technique would be of value clinically if the measurements could be made noninvasively in situ.

These new methods are quite promising for measuring the mechanical properties of tissues in vivo and advancing the materials science of collagenous tissues. However, for these techniques to provide accurate information about tissues they must consider nonlinear behavior, strain-rate dependence, and volumetric effects that occur during mechanical loading. It is well known that fluid flow during cartilage and bone deformation is an important mechanism for energy dissipation as well as a stimulator of tissue mechanotransduction (Kim et al., 1995; Fritton and Weinbaum, 2009). Fluid flow from tissues under load is an important contributor to nonlinear viscoelastic behavior. To ignore these effects limits the relevance of any technique used to determine the mechanical properties and limits the accuracy of the results obtained using these methods.

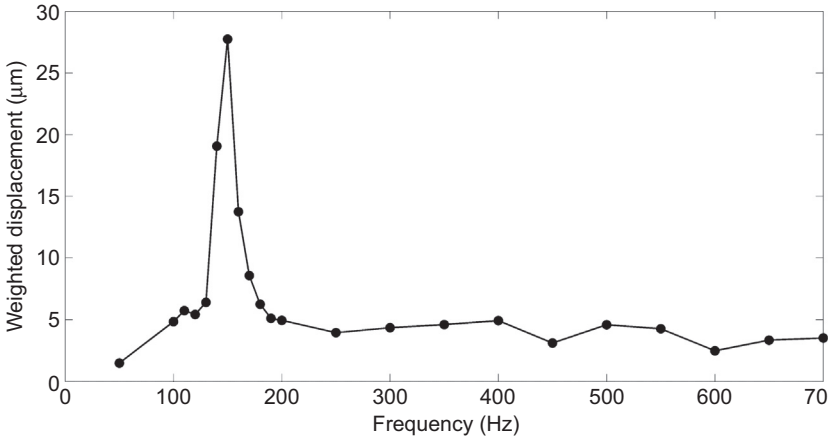

Figure 11.8 Vibrational analysis of decellularized dermis. A plot of weighted displacement versus vibration frequency is used to determine the resonant frequency. The resonant frequency is determined from measurement of the maximum displacement of a sample vibrated between 0 and 700 HZ. Note the maximum displacement is measured and converted into a vibrational modulus using the calibration curve shown in Fig. 11.9. The modulus measured at the resonant frequency is very close to the elastic modulus.
Reprinted from Shah R, Pierce MC, Silver FH: A method for non-destructive mechanical testing of tissues and implants, *J Biomed Mat Res Part A*, 2016.

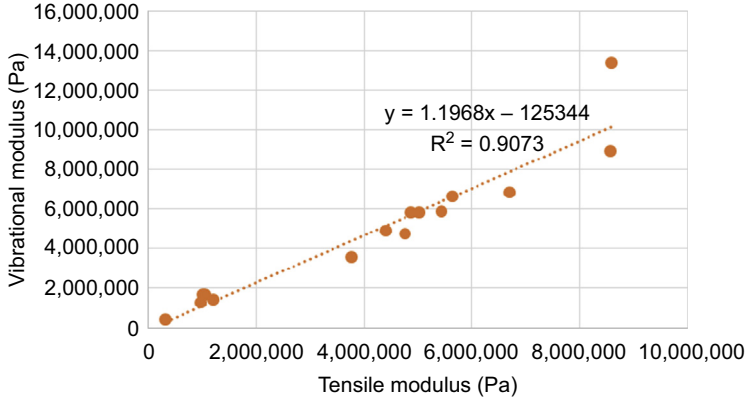

Figure 11.9 Typical calibration curve of modulus measured using vibrational method versus tensile modulus from conventional stress−strain testing in tension of human decellularized dermis. The modulus measured from the vibrational tests is obtained by determining the resonant frequency at which the maximum displacement of the sample occurs whilst the tensile modulus is obtained from the tangent to force versus extension curve. The slope of the plot is 11.9 suggesting that the modulus obtained from vibrational analysis is directly related to the tensile modulus.

11.10 Mechanotransduction

Collagen fibrils are a major factor in the conversion of mechanical forces and work into stored energy; in many cases this energy is stored in the form of high-molecular-weight polymers such as collagen fibers (Silver, 2006). When muscles and tendons are loaded, the muscle does work on the collagen fibers and energy is stored as work in the tendon. During tendon stretching the applied force stores work elastically, by stretching the triple helix; the energy is released after the load is removed.

Collagen fibrils are attached to cell membranes through attachment molecules such as integrins and other cell surface macromolecules. During this stretching of the collagen fibers, tension is transmitted through the cell membrane setting into motion the activation of the phosphorelay pathways inside the cell (Silver, 2006). Tension typically activates the MAP kinase pathways leading to synthesis of new collagen to "bolster" the ability of the tendons to support loads (Silver, 2006). Thus, some of the mechanical energy generated from the muscle tension is stored in the form of high−molecular-weight polymers; energy is stored in the form of covalent bonds that link amino acids together in the newly synthesized collagen fibers. When external tensile loads decrease, the collagen fibers atrophy and release the energy from the broken covalent bonds. This can occur during nonloading events, such as prolonged bed rest or when an astronaut is in a low gravitational field.

In this manner, collagen fibers are dynamic structures that are constantly growing or resorbing depending upon the level of tension they experience. The interactions between the collagen fibers and cells in tissues are an exciting part of the dynamics that occur in ECM biology that ultimately affects health and the pathogenesis of disease processes such as cancer.

11.11 Conclusions

Collagen fibers are the structural elements found in vertebrate tissues that transmit forces, store, and dissipate energy. Collagen fibers limit the deformation of tendon and other load bearing tissues and have a hierarchical structure that includes collagen molecules, microfibrils, fibrils, fibers, and fascicles. Collagen molecules are packed into a quarter-stagger arrangement with neighboring molecules staggered by multiples of D, which is about 22% of the molecular length. During mechanical deformation collagen molecules as well as the gap region of the D period are stretched. At larger strains, molecules and fibrils slide by each other, which leads to energy losses. Finally, collagen fiber failure occurs by disintegration of some of the hierarchical structure yielding collagen subfibrils that lose much of their mechanical strengths.

The ability of collagen-cell interactions to provide dynamic structural alterations in the mechanical properties of ECMs provides clinicians with the ability to monitor changes in tissue structure. However, this will require new techniques to measure changes in properties that occur during the disease process. For this to occur a detailed

understanding of collagen biomechanics is necessary since the time-dependence and deformation mechanism must be considered in order to provide accurate interpretations of the mechanical properties. This also requires the use of "gold standards" to make sure any new test developed can duplicate the behaviors that have been reported in the literature in the pioneering research of Yamada (1970) and Fung (1973).

Future studies are needed to identify the changes that occur in collagen fibers and their mechanical properties found in tissues that are associated with cancers and other pathologies (Dudea et al., 2013). Collagen fibers in ECMs are oriented in more than one direction and form multilayered sheets such as is observed in skin, cartilage, and bone. Changes in packing patterns and fiber orientation may be a useful criterion for early diagnosis of a number of disease states.

References

Birk DE, Silver FH, Trelstad RL: Matrix polymerization. In Hay ED, editor: *The cell biology of the extracellular matrix*, ed 2, NY, 1991, Academic Press, pp 221−254.

Diamant J, Keller A, Baer E, Litt M, Arridge RG: Collagen: ultrastructure and its relation to mechanical properties as a function of ageing, *Proc Roy Soc Lond B* 180:293−315, 1972.

Doyle BB, Hulmes DJ, Miller A, Parry DA, Piez KA, Galloway: A D-periodic narrow filament in collagen, *Proc R Soc Lond B* 186:67−74, 1974.

Drakonaki EE, Allen GM, Wilson DJ: Ultrasound elastography for musculoskeletal applications, *Br J Radiol* 85:1435−1445, 2012.

Dudea SM, Botar-Jid C, Dumitriu D, Vasillescu D, Manole S, Lenghel MI: Differentiating benign from malignant superficial lymph nodes with sonoelastography, *Med Ultrson* 15: 132−139, 2013.

Dunn MG, Silver FH: Viscoelastic behavior of human connective tissue: relative contribution of viscous and elastic components, *Connect Tissue Res* 12:59−70, 1983.

Folkhard W, Geercken W, Knorzer E, Mosler E, Nemetschekgansler H, Nemetschek T, Koch MHJ: Structural dynamic of native tendon collagen, *J Mol Biol* 193:405−407, 1987.

Fritton SP, Weinbaum S: Fluid and solute transport in bone: fluid induced mechanotransduction, *Annu Rev Fluid Mech* 41:347−374, 2009.

Fung YC: *Biomechanics: mechanical properties of living tissue,* ed 2, NY, 1973, Springer.

Horvath I, Foran DJ, Silver FH: Energy analysis of flow induced harmonic motion in blood vessel walls, *Cardiovasc Eng* 5:21−28, 2005.

Hulmes DJS: Collagen diversity, synthesis and assembly. In Fratzl P, editor: *Collagen, structure and mechanics*, New York, 2008, Springer, pp 15−47 (chapter 2).

Kennedy BF, Kennedy KM, Sampson DD: A review of optical coherence elastography: fundamentals, techniques and prospects, *IEEE J Sel Top Quan Electronics* 20, March/April 2014a.

Kennedy BF, McLaughlin RA, Kennedy KM, Chin L, Curatolo A, Tien A, Latham B, Saunders CM, Sampson DD: Optical coherence micro-elastography: mechanical-contrast imaging tissue microstructure, *Biomed Opt Express* 5:2113−2124, 2014b.

Ker RF: Damage and fatigue. In P Fratzl, editor: *Collagen, structure and mechanics*, New York, 2008, Springer, pp 11−131 (chapter 5).

Ker RF, Wang XT, Pike AVL: Fatigue quality of mammalian tendons, *J Exp Biol* 203: 1317−1327, 2000.

Kim Y-J, Bonassar J, Grodzinsky AJ: The role of cartilage streaming potential, fluid flow and pressure in the stimulation of chondrocyte biosynthesis during dynamic compression, *J Biomechanics* 28:1055−1066, 1995.

Low G, Kruse SA, Lomas DJ: General review of magnetic resonance elastography, *World J Radiol* 8(1):59−72, 2016.

McBride DJ, Hahn R, Silver FH: Morphological characterization of tendon development during chick embryogenesis: measurement of birefringence retardation, *Int J Biol Macromol* 7: 71−76, 1985.

McBride DJ, Trelstad RL, Silver FH: Structural and mechanical assessment of developing chick tendon, *Int J Biol Macromol* 10:194−200, 1988.

Panjabi MM, Yoldas E, Oxland TR, Crisco 3rd JJ: Subfailure injury of the rabbit anterior cruciate ligament, *J Orthopaedic Res* 14:216−222, 1996.

Panjabi MM, Moy P, Oxland TR, Cholewicki J: Subfailure injury affects the relaxation behavior of rabbit ACL, *Clin Biomech* 14:24−31, 1999.

Parry DA, Barnes GR, Craig AS: A comparison of the size distribution of collagen fibrils in connective tissues as a function of age and a possible relation between fibril size distribution and mechanical properties, *Proc R Soc Lond B Biol Sci* 203:293−303, 1978.

Pease DC, Bouteille M: The tridimensional ulttrastructure of native collagen fibrils, cytochemical evidence for a carbohydrate matrix, *J Ultrastur Res* 35:339−358, 1972.

Pins GD, Huang EK, Christiansen DL, Silver FH: Effects of axial static strain on the tensile properties and failure mechanisms of self-assembled collagen fibers, *J Appl Polym Sci* 63: 1429−1440, 1997.

Provenzano PP, Hayashi K, Kunz DN, Markel MD, Vanderby Jr R: Healing of subfailure ligament injury: comparison between immature and mature ligaments in a rat model, *J Orthopaedic Res* 20:975−983, 2002a.

Provenzano PP, Heisey D, Hayashi H, Lakes R, Vanderby Jr R: Subfailure damage in ligament: a structural and cellular evaluation, *J Appl Physiol* 92:362−371, 2002b.

Provezano PP, Alejandro-Osorio AL, Valhmu WB, Jensen KT, Vanderby Jr R: Intrinsic fibroblast-mediated remodeling of damaged collagenous matrices in vivo, *Matrix Biol* 23: 543−555, 2005.

Ricard-Blum S: The collagen family. In Hynes R, Yamada K, editors: *Cold spring harbor perspectives in biology*, 2011, pp 1−19.

Ruberti JW, Roy AS, Roberts CJ: Corneal biomechanics and biomaterials, *Annu Rev Biomed Eng* 13:269−295, 2014.

Sasaki N, Shukunami N, Matsushima N, Izumi Y: Time-resolved X-ray diffraction from tendon collagen during creep using synchrotron radiation, *J Biomech* 32:285−292, 1999.

Scott JE: Supramolecular organization of extracellular matrix glycosaminoglycans in vitro and in tissues, *FASEB J* 6:2639−2645, 1992.

Shah R, Pierce MC, Silver FH: A method for non-destructive mechanical testing of tissues and implants, *J Biomed Mat Res A*, 2016.

Silver FH: *Mechanosensing and mechanochemical transduction in extracellular matrix, biological, chemical, engineering and physiological aspects*, New York, 2006, Springer.

Silver FH, Horvath I, Foran DJ: Mechanical implications of the domain structure of fibril forming collagens: comparison of molecular and fibrillar flexibility of ∝-chains found in types I, II and III collagens, *J Theo Biol* 216:243−254, 2002.

Silver FH, Landis WJ: Viscoelasticity, energy storage and transmission and dissipation by extracellular matrices in vertebrates. In Fratztl P, editor: *Collagen, structure and mechanics*, New York, 2008, Springer, pp 133−154 (chapter 6).

Silver FH, Langley KH, Trelstad RL: Linear aggregation and the turbidimetric lag phase: type I collagen fibrillogenesis in vitro, *J Theo Biol* 81:515−526, 1979.

Silver FH, Kato YP, Ohno M, Wasserman AJ: Analysis of mammalian connective tissue: relationship between hierarchical structures and mechanical properties, *J Long Term Eff Med Implants* 2:165−172, 1992.

Silver FH, Christiansen DL, Snowhill P, Chen Y: Role of storage on changes in the mechanical properties of tendon and self-assembled collagen fibers, *Connect Tissue Res* 41:155−164, 2000.

Silver FH, Christiansen DL, Snowhill PB, Chen Y: Transition from viscous to elastic−based dependency of mechanical properties of self-assembled type I collagen fibers, *J Appl Polym Sci* 79:134−142, 2001.

Silver FH, Freeman JW, Seehra GP: Collagen self-assembly and development of matrix mechanical properties, *J Biomech* 36:1529−1553, 2003.

Smith JW: Molecular pattern in native collagen, *Nature* 219:157−158, 1968.

Song S, Le NM, Huang Z, Shen T, Wang RK: Quantitative shear-wave optical coherence elastography with a programmable phased array ultrasound as the wave source, *Opt Lett* 40(21):5007−5010, 2015.

Torp S, Baer E, Friedman B: Effects of Age and of mechanical deformation on the ultrastructure of tendon. In , UK, 1974, University of Bristol, pp 223−250. *Proceedings of the colston conference*, vol. 26. UK, 1974, University of Bristol, pp 223−250.

Wang S, Larin KV: Optical coherence elastography for tissue characterization: a review, *J Biophotonics* 8(4):279−302, 2015.

Yahia L, Brunet J, Labelle S, Rivard CH: A scanning electron microscopic study of rabbit ligaments under strain, *Matrix* 10:58−64, 1990.

Yamada H: *Strength of biological materials*, Baltimore, MD, 1970, Williams and Wilkins.

Zaleska-Dorobisz U, Kaczorowski K, Pawlus A, Puchalskoc A, Inglot M: Ultrasound elastography-review of techniques and its clinical application, *Adv Clin Exp Med* 23(4): 645−655, 2014.